Jurnal Teknik Informatika (JUTIF)
P-ISSN: 2723-3863
E-ISSN: 2723-3871
Vol. 7, No. 3, June 2026, Page. 2588-2599
https://jutif.if.unsoed.ac.id
DOI: https://doi.org/10.52436/1.jutif.2026.7.3.5554

Oil Palm Stem Disease Detection Based on Color Moments and GLCM Texture Features Using Artificial Neural Networks

Hamdani Hamdani[1], Anindita Septiarini[*2], Encik Akhmad Syaifudin[3], Andi Tejawati[4], Muhammad Zulfariansyah[5]

[1,2,4]Department of Informatics, Faculty of Engineering, Mulawarman University, Samarinda, Indonesia
[3]Faculty of Agriculture, Mulawarman University, Samarinda, Indonesia
[5]Department of Information System, Faculty of Engineering, Mulawarman University, Samarinda, Indonesia

Email: [2]anindita@unmul.ac.id

Received : Dec 10, 2025; Revised : Jan 26, 2026; Accepted : Jan 26, 2026; Published : Jun 15, 2026

Abstract

Oil palm is an essential commodity for the economy; however, basal stem rot caused by Ganoderma boninense poses a significant threat to plantation productivity and long-term vitality. It highlights the importance of early detection of stem disease to facilitate timely intervention and minimize potential economic losses. This study presents an image-based approach to diagnosing oil palm stem maladies, leveraging handcrafted color and texture features within a supervised machine learning framework. The dataset contained 525 images of oil palm stems, of which 205 depicted healthy specimens, and 320 depicted diseased ones. These were captured within their natural environment. Color features were derived by analyzing color moments within the HSV color space, while texture features were extracted from the Grey-Level Co-occurrence Matrix (GLCM). The extracted features were classified employing an Artificial Neural Network (ANN) and were subsequently contrasted with classifiers including Decision Tree, K-Nearest Neighbors, Naive Bayes, and Support Vector Machine. Model performance was evaluated using k-fold cross-validation with k = 5 and k = 10 to ensure the consistency and reliability of the assessment. The experimental results demonstrated that the highest accuracy of 97.52% was achieved when the ANN model was used to classify the integrated color and texture features. The innovative aspect of this research resides in demonstrating that handcrafted features integrated with artificial neural networks can attain high detection accuracy in scenarios with limited data, providing a viable alternative to data-intensive deep learning techniques. This method facilitates a dependable, computer vision-driven early detection system for oil palm stem diseases, thereby promoting sustainable plantation management.

Keywords : *Artificial Neural Network, Color Feature, Cross Validation, Plant Disease Detection, Texture Feature.*

1. INTRODUCTION

Indonesia is one of the countries in the Southeast which is a major producer of palm oil products. These products have been instrumental in eradicating poverty in these countries [1] and provide a valuable source of foreign exchange revenues [2]. The oil palm business is rapidly gaining popularity and becoming a well-known company. It is sometimes referred to as the "golden crop of Indonesia." Oil palm is a substantial agricultural commodity in Southeast Asia, contributing one-third of the global supply of vegetable oil and fat [3]. Indonesia and Malaysia collectively produce 85% of the world's palm oil, with 75% intended for food consumption and the remaining fraction for industrial use. Indonesia was the primary producer in 2019, accounting for 42.5 million tonnes, which accounts for 58% of the global supply. Riau province accounted for 9.12 million tonnes of the 45.86 million tonnes of palm oil produced in 2019 [4], Indonesia's highest proportion of palm oil output.

Vol. 7, No. 3, June 2026, Page. 2588-2599
https://jutif.if.unsoed.ac.id
DOI: https://doi.org/10.52436/1.jutif.2026.7.3.5554

Palm oil and products derived from palm are among the nation's top 10 exports, and they have experienced consistent annual growth over the past three decades. The disease of basal stem rot (BSR) is caused by Ganoderma boninense, a white-rot fungus [5]. Basal stem rot (BSR) is caused by the fungus Ganoderma boninense, which decomposes wood. It is caused by a fungal mycelia invasion that spreads to the plant's bole. BSR spreads through airborne basidiospores and direct contact with infected roots. These fungi usually break down cell wall components, such as lignins. The BSR reduces the output of oil palm fresh fruit bunches (FFB) and causes the palms to collapse [6]. The first stage of BSR infection entails the fungus infiltrating and breaking down the cell wall of the oil palm tree, therefore intercepting vital nutrients. When first examined, the tree exhibits little indication of disease. As the infection advances, leaves exhibit chlorosis, and symptoms manifest at the affected shoot. The tree's foliage undergoes elongation into spear-like structures and then becomes yellow. The tree's base darkens due to stem deterioration, and basidiocarps are frequently present near the root. Detachment of the upper portion results in the tree's collapse [7].

Investigation into image processing and computer vision in agriculture has been implemented on several plant species, including land decision [8], fruit [9]–[11], leaves [12]–[14], and plant stems [3], [5]. In the realm of computer vision and machine learning, the identification of illnesses in plants has shown encouraging outcomes in recent times. Several works have applied machine learning for classification to develop computer vision implementation, but many still discuss plant stem diseases.

Fungi, bacteria, and viruses are the primary perpetrators of most plant illnesses, a critical area of research for plant automatic disease detection. The experimental results illustrate the proposed model's superior performance compared to pre-trained models like InceptionV3 and VGG16. The classification result ranges from 76% to 100% [15]. A recent study analyzed several networks to detect plant diseases and pests in some plants. The networks consisted of classification, detection, and segmentation modules. This study observed a positive correlation between the implementation of EPOCH algorithms and the accuracy of the Inception V3 model, which gets 95% accuracy in determining diseases [16].

The deep learning-enabled object detection model was applied for multi-class plant disease and has been proposed based on a state-of-the-art computer vision algorithm. This proposed model has been improved to optimize detection speed and accuracy and applied to multi-class apple plant disease detection in the real environment. The mean average precision (mAP) and F1-score of the detection model reached 91.2% and 95.9%, respectively, at a detection rate of 56.9 FPS. The overall detection result demonstrates that the current algorithm significantly outperforms the state-of-the-art detection model with a 9.05% increase in precision and a 7.6% increase in F1-score [17]. Furthermore, deep learning recognizes plant diseases, specifically apples, corn, grapes, potatoes, sugarcane, and tomatoes. The system can also detect several diseases of plants. Comprised of 35,000 images of healthy plant leaves and infected with the diseases. The trained model has achieved an accuracy rate of 96.5%, and the system could register up to 100% accuracy in detecting and recognizing the plant variety and the type of diseases the plant was infected with [18].

An intelligent technique was proposed using a Random Forest classifier to detect leaves and plants such as apples, Corn, Grapes, potatoes, and Tomatoes with 93% average accuracy from all the datasets [19]. Subsequently, computer vision technology and machine learning were applied to develop disease detection techniques for oil palms, and the Deep Learning Alexnet CNN model was created, which accurately detects illnesses in palm oil leaves without manual feature extraction. The AlexNet-SVM model, in which AlexNet CNN was utilized as the feature extractor of SVM, was applied to solve the oil palm leaf disease classification. The performance of the classification models was evaluated based on accuracy, precision, recall, specificity, and F1 score. The average accuracy, precision, recall, specificity, and F1-score of 0.98, 0.96, 0.99, 0.96, and 0.96, and 0.96, 0.91, 0.97, 0.92, and 0.92 were attained by AlexNet CNN and AlexNet-SVM, respectively [20]. The Yolov5 model was used to assess

Vol. 7, No. 3, June 2026, Page. 2588-2599
https://jutif.if.unsoed.ac.id
DOI: https://doi.org/10.52436/1.jutif.2026.7.3.5554

oil palm tree well-being based on aerial pictures, achieving exceptional precision in detection and classification. The image data are divided into five classes: healthy, smallish, yellowish, mismanaged, and dead palms. This study achieves an average Fl-score of 0.895, outperforming Faster R-CNN (0.706) and CNN ResNet-101 (0.493). The strength of the YOLOv5 model is high precision for all five classes, which is above 0.961. This application provides fast, robust, and accurate oil palm tree counting that can be applied elsewhere globally [21].

Deep learning methods have significant potential; however, they pose many challenges when applied to real-world farming settings. Most of the time, these methods require large labeled datasets, substantial computing power, and long training times. In scenarios where datasets are limited—such as stem-based oil palm disease images captured under field conditions—deep learning models are prone to overfitting and reduced generalization performance [19]–[21]. Furthermore, most existing studies primarily focus on leaf-based disease detection. At the same time, relatively limited attention has been given to stem-based disease detection, which is crucial for identifying basal stem rot at an earlier stage [22]–[24].

Applying constructed color and texture features, along with supervised machine learning classifiers, is a lightweight, computationally effective method for analyzing images when sufficient information is unavailable. Methods based on color moments and the GLCM have been shown to effectively capture visual features related to disease. Yet, their integration with simple and effective classifiers, including Artificial Neural Networks, for oil palm stem disease detection remains underexplored [25]–[28]. The majority of studies have focused on leaf-based detection or deep learning methods. A few studies have investigated stem-based disease detection that uses custom features and lightweight classifiers. To develop detection systems that work in plantation environments with limited resources, it is important to address this gap.

This study aimed to develop an image-based oil palm stem disease detection system using color moments and GLCM texture features, with classification performed by an ANN. The discriminative features were extracted from stem images, and the ANN's classification performance was tested against other supervised machine learning classifiers using comparable validation methods on a limited dataset. This work is exciting because the results show that constructing color and texture features with an ANN can achieve high detection accuracy without requiring extensive data for deep learning models. This study contributes to the development of an efficient and reliable computer vision-based early detection system for oil palm stem diseases, supporting sustainable plantation management and practical field deployment.

2. METHOD

This study presents a computer vision–driven machine learning framework for identifying diseases in oil palm stems. Image acquisition, preprocessing, feature extraction, classification, and performance evaluation were all components of the overall method. The workflow was designed to identify unique visual features in stem images while still running quickly, even with limited data. Figure 1 shows the overall approach framework.

2.1. Dataset

Image data were acquired using a Canon EOS 550D digital camera to capture oil palm stem images under natural field conditions. Image acquisition was conducted outdoors under stable weather conditions with sufficient natural illumination to minimize shadow effects and lighting variability. The camera was positioned at a distance of approximately 20–40 cm from the stem surface, with the camera lens oriented perpendicular to the trunk to ensure consistent texture representation. All images were captured at 5184 × 3456 pixels. The dataset consists of 525 oil palm stem images, comprising 205

Vol. 7, No. 3, June 2026, Page. 2588-2599
https://jutif.if.unsoed.ac.id
DOI: https://doi.org/10.52436/1.jutif.2026.7.3.5554

healthy samples and 320 infected samples. The dataset includes variations in stem appearance, orientation, and disease severity to improve model generalization. Representative examples of healthy and infected stem images are shown in Figure 2.

2.2. Pre-processing

Pre-processing was applied to enhance image quality and standardize visual characteristics prior to feature extraction. Initially, RGB images were converted to grayscale for texture analysis. Contrast stretching was then applied to improve the visibility of disease-related patterns on the stem surface. In addition, RGB images were transformed into the HSV color space to facilitate robust color feature extraction. The HSV representation was selected because it separates chromatic information from illumination, making it more resilient to lighting variations commonly encountered in outdoor environments [22]. The resulting grayscale enhancement and HSV transformation outputs are illustrated in Figure 3.

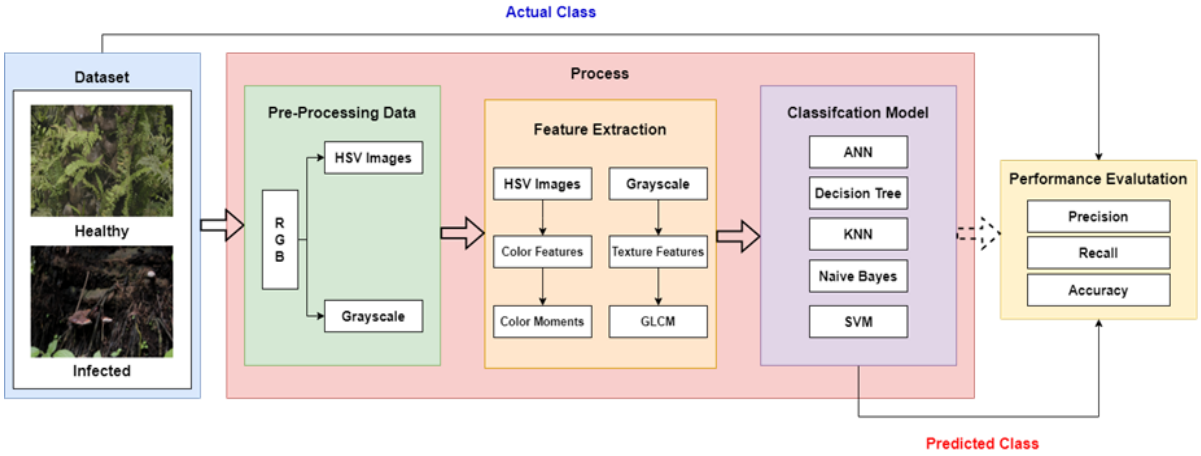

Figure 1. The methodology of oil palm stem disease detection.

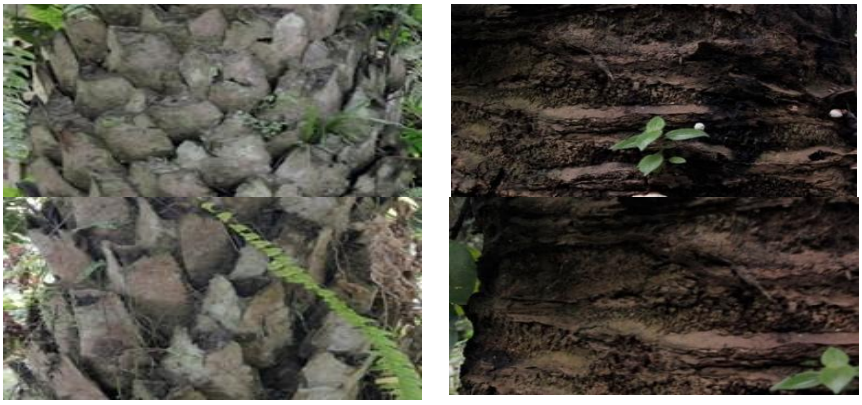

(a) (b)

Figure 2. The example image in the dataset of each class: (a) healthy and (b) Infected.

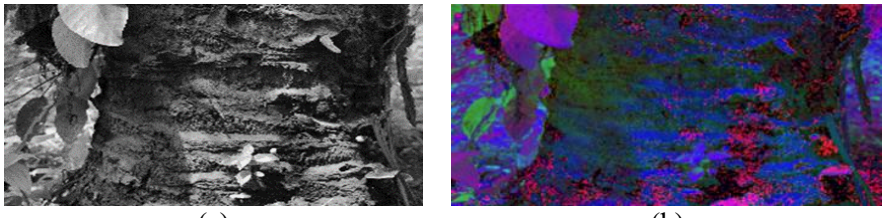

(a) (b)

Figure 3. The resulting image in pre-processing: (a) contrast stretching and (b) HSV color space

Vol. 7, No. 3, June 2026, Page. 2588-2599
https://jutif.if.unsoed.ac.id
DOI: https://doi.org/10.52436/1.jutif.2026.7.3.5554

2.3. Feature Extraction

This investigation employed the color moments method to compare two color spaces, RGB and HSV. This procedure converts the RGB to HSV color space to restrict the color gamut's dimensions and properties. The GLCM was employed to extract texture features, and its efficacy was contrasted to that of the color moments method, which applied the RGB to the HSV color model.

2.3.1. Color Feature

The color moment was implemented due to a highly straightforward and efficient color characteristic [23], [24]. The underlying mathematical principle of this method is that the distribution of colors in an image may be accurately described using its moments. Since the color distribution information primarily focuses on the lower-order moments, only a color's mean, variance, and skewness are necessary to represent the image's color distribution. The formulations of the three-color moments with low order are defined in equations (1)-(3) [25].

$$\mu_i = \frac{1}{N}\sum_{j=1}^{N} P_{ij} \quad , i = 1,2,3 \tag{1}$$

$$\sigma_i = \left(\frac{1}{N}\sum_{j=1}^{N}\left(P_{ij} - \mu_i\right)^2\right)^{1/2} \quad , i = 1,2,3 \tag{2}$$

$$s_i = \left(\frac{1}{N}\sum_{j=1}^{N}\left(P_{ij} - \mu_i\right)^3\right)^{1/3} \quad , i = 1,2,3 \tag{3}$$

2.3.2. Texture Feature

Texture characteristics were extracted using the Grey-Level Co-occurrence Matrix (GLCM), a statistical method for modeling spatial relationships between pixel intensities in grayscale images. By capturing surface irregularities caused by stem degradation, GLCM features offer effective texture analysis. In this work, four features—Contrast (B1), Correlation (B2), Energy (B3), and Homogeneity (B4)—were extracted at four orientations (0°, 45°, 90°, 135°) with a fixed pixel distance, following Equations (4)–(7) [26], resulting in 20 texture features per image. Combined with six color features, each image yielded 26 features. Table 1 presents examples of features for healthy and infected samples.

$$B1 = \sum_{i,j}(i-j)^2 P(i,j) \tag{4}$$

$$B2 = \frac{\sum_{i,j}(i.j)P(i,j) - \mu_i\mu_j}{\sigma_i\sigma_j} \tag{5}$$

$$B3 = \sum_{i,j} P(i,j)^2 \tag{6}$$

$$B4 = \sum_{i,j}\frac{P_{ij}}{1+(i-j)^2} \tag{7}$$

All extracted features were normalized using min-max scaling prior to classification to ensure that each feature contributed equally to the learning process. This approach is essential for distance-based classifiers and neural networks because unscaled features can bias the training process toward attributes with larger numeric ranges.

Vol. 7, No. 3, June 2026, Page. 2588-2599
https://jutif.if.unsoed.ac.id
DOI: https://doi.org/10.52436/1.jutif.2026.7.3.5554

Table 1. The Example of Feature Extraction Results

Stem image	Feature	
	Color	Texture
 Healthy	μH: 0.1979 μS: 0.2271 μV: 0.5909	$B1^{0}$: 1,1924 $B1^{45}$: 0.8291 $B1^{90}$:0.0623 $B1^{135}$:0.0727 $B2^{0}$: 1.3134 $B2^{45}$:0.8116 $B2^{90}$:0.0594 $B2^{135}$:0.7131 $B3^{0}$: 1.1033 $B3^{45}$:0.8421 $B3^{90}$:0.0658 $B3^{135}$:0.7425 $B4^{0}$: 1.3126 $B4^{45}$:0.8117 $B4^{90}$:0.0594 $B4^{135}$:0.7115
 Infected (Ganoderma)	μH: 0.3067 μS: 0.1661 μV: 0.1991	$B1^{0}$: 0.62255 $B1^{45}$: 0,8283 $B1^{90}$:0,1841 $B1^{135}$: 0,8162 $B2^{0}$: 0,7161 $B2^{45}$: 0,8032 $B2^{90}$:0,1793 $B2^{135}$: 0,8031 $B3^{0}$: 0,6081 $B3^{45}$: 0,8327 $B3^{90}$:0,1923 $B3^{135}$: 0,8257 $B4^{0}$: 0,8619 $B4^{45}$: 0,7631 $B4^{90}$:0,1695 $B4^{135}$: 0,7848

2.4. Classsification

Five supervised machine learning algorithms were used to classify the normalized feature vectors: Artificial Neural Network (ANN) [26], Decision Tree [27], K-Nearest Neighbors (KNN) [28], Support Vector Machine (SVM) [29], and Naive Bayes [30]. The selection of these classifiers enables a comprehensive comparison of probabilistic, distance-based, tree-based, margin-based, and neural network methods.

The ANN classifier was implemented using a feedforward multilayer perceptron architecture. The model consists of an input layer with 26 neurons representing the extracted features, a single hidden layer with 16 neurons, and an output layer with two neurons corresponding to the healthy and infected classes. The number of neurons in the hidden layer was selected based on empirical testing to achieve an appropriate balance between model complexity and generalization. Training was performed using the backpropagation algorithm, with a learning rate of 0.01 and a maximum of 1,000 epochs. The hidden layer utilized a sigmoid activation function, while the output layer employed a softmax function. Hyperparameters were determined through preliminary experiments to promote stable convergence and optimal classification accuracy.

Vol. 7, No. 3, June 2026, Page. 2588-2599
https://jutif.if.unsoed.ac.id
DOI: https://doi.org/10.52436/1.jutif.2026.7.3.5554

The KNN classifier was configured by empirically selecting the value of k that resulted in the lowest classification error. The SVM employed an radial basis function (RBF) kernel, with penalty and kernel parameters optimized through experimental tuning. The decision tree and Naive Bayes classifiers were implemented with default parameter settings to minimize the risk of overfitting.

2.5. Performance Evaluation

Model performance was assessed using precision, recall, and accuracy metrics. To provide a reliable and unbiased evaluation, k-fold cross-validation was implemented with k values of 5 and 10 [31]. The choice of these k values represents a balance between computational efficiency at k = 5 and enhanced estimation stability at k = 10. Consistent performance across both folds demonstrates model robustness and reduces the risk of overfitting. Classification outcomes were examined for color, texture, and combined feature sets.

3. RESULT

The approach suggested was able to achieve the highest level of accuracy. Consequently, numerous experiments were conducted to substantiate the appropriate method for the dataset employed in this investigation. The method evaluation was performed using a variety of feature sets, such as color features, texture features, and both features. These feature sets were fed into five classifiers: ANN, Decision Tree, KNN, Naive Bayes, and SVM. The classification was conducted through cross-validation, with a dataset comprising 525 images (205 infected and 320 uninfected). The k-fold value was set to 5 and 10. Three evaluation parameters were employed to evaluate the method's performance: precision (p), recall (r), and accuracy (a) in percentage. Tables 2–4 summarise the test results for each classifier using the diverse feature sets obtained.

Table 2. The Performance Comparison of The Classifier Using Color and Texture Features Set

Classifier	K-fold = 5			K-fold = 10		
	p(%)	r(%)	a(%)	p(%)	r(%)	a(%)
ANN	97.00	97.00	96.95	97.50	97.50	97.52
Decision Tree	86.60	86.70	86.67	86.60	86.70	86.67
KNN	95.60	95.60	95.61	95.60	95.60	95.61
Naive Bayes	74.70	74.90	74.85	74.70	74.90	74.85
SVM	96.90	97.00	96.95	96.90	97.00	96.95

Table 3. The Performance Comparison of The Classifier Using Color Feature Set

Classifier	K-fold = 5			K-fold = 10		
	p(%)	r(%)	a(%)	p(%)	r(%)	a(%)
ANN	81.90	81.90	81.9	82.60	82.80	82.70
Decision Tree	79.10	79.20	79.23	80.60	80.50	80.57
KNN	80.00	80.02	80.19	80.00	80.20	80.19
Naive Bayes	74.50	74.70	74.66	73.30	73.50	73.52
SVM	81.00	81.00	80.95	81.20	81.10	81.14

Table 4. The Performance Comparison of The Classifier Using Texture Feature Set

Classifier	K-fold = 5			K-fold = 10		
	p(%)	r(%)	a(%)	p(%)	r(%)	a(%)
ANN	97.40	97.30	97.33	97.40	97.30	97.33
Decision Tree	84.00	84.00	84.00	86.00	85.70	85.71
KNN	93.60	93.50	93.52	94.30	94.30	94.28
Naive Bayes	72.70	72.80	72.76	72.20	72.40	72.38
SVM	96.10	96.00	96	96.10	96.00	96.00

Vol. 7, No. 3, June 2026, Page. 2588-2599
https://jutif.if.unsoed.ac.id
DOI: https://doi.org/10.52436/1.jutif.2026.7.3.5554

Table 2 shows that combining color and texture features yielded the highest performance across all classifiers. The ANN classifier achieved the best results. It achieved accuracies of 96.95% for k = 5 and 97.52% for k = 10, while maintaining balanced precision and recall. SVM achieved accuracy values similar to ANN, but ANN showed greater consistency across validation folds. Naive Bayes yielded the lowest performance, reflecting its limited capacity to capture complex feature relationships.

The classification results using only color features, as shown in Table 3, indicate lower overall performance than those with the combined feature set. This finding suggests that color information alone does not adequately capture stem disease patterns. ANN and SVM both achieved accuracy levels above 81%. Decision Tree and KNN produced moderate results. Naive Bayes again recorded the lowest accuracy, underscoring its sensitivity to limited discriminative input.

Table 4 presents the results using texture features, which show a marked improvement in classification performance compared to color-only features. The ANN classifier achieved consistently high accuracy of 97.33% for both k = 5 and k = 10, supporting the effectiveness of GLCM-based texture descriptors in distinguishing stem conditions. SVM also performed at a comparable level, while Decision Tree and KNN achieved intermediate results. These findings indicate that texture features are critical for distinguishing healthy from infected stem surfaces.

In all experimental settings, the ANN classifier either outperformed the other models or achieved similar accuracy with lower variance across validation folds. This indicates strong generalization capability. The consistent results observed between k = 5 and k = 10 suggest the approach is stable with respect to data partitioning and demonstrates reduced risk of overfitting. Ensure that peak accuracy values were not overinterpreted; assess performance stability by examining metric variation across validation folds. The ANN classifier showed minimal variation between k = 5 and k = 10, with accuracy differences remaining below 1%, which indicates low variance and stable generalization. In comparison, Decision Tree and Naive Bayes exhibited greater fluctuations in performance across folds. These results suggest that ANN provides more reliable classification performance, particularly with limited datasets.

ANN exhibits outstanding performance in terms of texture features, particularly when assessed by cross-validation with the k-fold value of 10. The SVM is competitive, exhibiting high values comparable to the ANNs. Compared to Naive Bayes, Decision Tree, and KNN demonstrate higher performance, attaining accuracy above 72%. The confusion matrix assesses the capacity of a model to differentiate between hypothetical situations of good health and those of infection. The program achieved a 97.07% accuracy in accurately identifying 199 healthy samples but misclassified only six diseased samples. The model attained a precision rate of 97.81% by accurately detecting 313 out of 320 samples specifically classified as infected. The model attains a cumulative accuracy rate of 97.52% with a margin of error of 2.48%. Implementing the textural feature enables the successful distinction between healthy and sick samples. The K-Fold 10 validation criterion guarantees the absence of overfitting and enables efficient extrapolation to new data. Figure 4 presents the confusion matrix outcomes obtained from ANN that incorporate color and texture features using the k-fold value of 10 validation method.

Figure 4 further confirms the effectiveness of the ANN classifier. Using combined color and texture features with k = 10 cross-validation, the model correctly classified 199 out of 205 healthy samples, with only six misclassifications. For infected samples, 313 of 320 images were correctly identified, yielding a precision of 97.81% for the infected class. These results demonstrate that the proposed method maintains balanced performance across classes and does not bias toward the majority class. A quantitative comparison between ANN and SVM indicates that both classifiers achieved high performance; however, ANN consistently provided slightly higher accuracy and recall across all feature sets. For combined features with k = 10, ANN achieved an accuracy of 97.52%, marginally outperforming SVM at 96.95%. More importantly, ANN demonstrated greater stability across validation

Vol. 7, No. 3, June 2026, Page. 2588-2599
https://jutif.if.unsoed.ac.id
DOI: https://doi.org/10.52436/1.jutif.2026.7.3.5554

folds, whereas SVM exhibited minor performance fluctuations. This suggests that ANN offers better robustness for stem-based disease detection under limited data scenarios.

TARGET / OUTPUT	Healthy	Infected	SUM
Healthy	199 37.90%	6 1.14%	205 97.07% 2.93%
Infected	7 1.33%	313 59.62%	320 97.81% 2.19%
SUM	206 96.60% 3.40%	319 98.12% 1.88%	512 / 525 97.52% 2.48%

Figure 4. Confusion matrix of using ANN classifiers using cross-validation with a k-fold value of 10

4. DISCUSSIONS

The integration of color moments and GLCM texture features was found to improve the robustness of oil palm stem disease detection. Among the classifiers assessed, the Artificial Neural Network (ANN) achieved the highest accuracy, precision, and recall in both 5-fold and 10-fold cross-validation. These results indicate that ANNs are effective in capturing the nonlinear relationships within combined color and texture feature spaces. Compared to Decision Tree, KNN, and Naive Bayes classifiers, ANN exhibited greater stability and generalization, while SVM achieved similar but slightly lower performance.

In comparison to deep learning approaches reported in previous studies, the proposed method achieved comparable accuracy while utilizing fewer computational resources. For example, CNN-based models such as AlexNet and YOLOv5 reported accuracies above 95% for oil palm leaf disease detection and tree health monitoring [20], [21], but required large datasets and high-performance hardware. The present approach, which relies on handcrafted features, attained 97.52% accuracy using 525 stem images, indicating effectiveness under limited data conditions. These findings suggest that engineered features combined with ANN offer a practical alternative to deep learning, particularly for stem-based disease detection with limited annotated data.

The results of this study demonstrate that classical image features continue to be relevant for agricultural applications when systematically designed and evaluated. While recent research frequently emphasizes deep learning architectures, the findings indicate that lightweight supervised models can achieve competitive performance for early disease detection. Most existing studies focus on leaf-based analysis, whereas the present work addresses stem-based detection, which is critical for the early identification of basal stem rot. The proposed method broadens the application of computer vision techniques in agricultural informatics, particularly in plantation environments with limited computational resources.

Several limitations should be acknowledged. The dataset was collected under a single acquisition setting, which may restrict the model's generalizability to different plantation conditions, lighting environments, or camera devices. Although k-fold cross-validation was employed to address overfitting, the model has not been validated on an independent external dataset. Additionally, the study is limited to binary classification (healthy versus infected) and does not account for varying levels of disease severity. These factors may influence external validity and warrant further investigation before large-scale implementation.

Vol. 7, No. 3, June 2026, Page. 2588-2599
https://jutif.if.unsoed.ac.id
DOI: https://doi.org/10.52436/1.jutif.2026.7.3.5554

5. CONCLUSION

This study contributes to the field of plant disease detection by demonstrating that a combination of handcrafted color moments and GLCM texture features, together with an Artificial Neural Network, can achieve accurate and reliable detection of oil palm stem diseases under limited data conditions. Unlike most existing studies, which predominantly focus on leaf-based detection or rely on data-intensive deep learning models, this work emphasizes stem-based disease detection using a lightweight supervised learning framework better suited to practical plantation environments. Experimental results confirmed that the integrated color and texture features classified by the ANN achieved the highest performance, with accuracy, precision, and recall reaching 97.52%, and were consistently validated using k-fold cross-validation with k = 5 and k = 10. These findings highlight the practical significance of engineered features in mitigating overfitting risks while maintaining high classification performance when large-scale datasets are unavailable. From an application perspective, the proposed approach offers a computationally efficient, interpretable solution that supports early disease detection and timely intervention in oil palm plantations. Future work may extend this framework toward real-time or mobile-based detection systems, incorporate disease severity grading, and evaluate robustness under more diverse field conditions to further enhance its applicability and impact.

ACKNOWLEDGEMENT

The authors gratefully acknowledge the Faculty of Engineering, Universitas Mulawarman, for its support and facilitation throughout the completion of this research.

REFERENCES

[1] R. Nabila, et al., “Oil palm biomass in Indonesia: Thermochemical upgrading and its utilization,” Renewable and Sustainable Energy Reviews, vol. 176, no. April, p. 113193, 2023. https://doi.org/10.1016/j.rser.2023.113193.

[2] R. Hushiarian, N. A. Yusof, and S. W. Dutse, “Detection and control of Ganoderma boninense: Strategies and perspectives,” Springerplus, vol. 2, no. 1, pp. 1–12, 2019. https://doi.org/10.1186/2193-1801-2-555.

[3] Y. Siddiqui, A. Surendran, R. R. M. Paterson, A. Ali, and K. Ahmad, “Current strategies and perspectives in detection and control of basal stem rot of oil palm,” Saudi J. Biol. Sci., vol. 28, no. 5, pp. 2840–2849, 2021. https://doi.org/10.1016/j.sjbs.2021.02.016.

[4] H. Varkkey, A. Tyson, and S. A. B. Choiruzzad, “Palm oil intensification and expansion in Indonesia and Malaysia: Environmental and socio-political factors influencing policy,” Forest Policy and Economics, vol. 92, no. July, pp. 148–159, 2018. https://doi.org/10.1016/j.forpol.2018.05.002

[5] N. A. Husin, S. Khairunniza-bejo, and A. F. Abdullah, “Classification of Basal Stem Rot Disease in Oil Palm Plantations Using Terrestrial Laser Scanning Data,” Agronomy, p. 10, 2020. https://doi.org/10.3390/agronomy10111624.

[6] M. Sahebi et al., “Profiling secondary metabolites of plant defence mechanisms and oil palm in response to Ganoderma boninense attack,” International Biodeterioration & Biodegradation, vol. 122, no. August, pp. 151–164, 2017. https://doi.org/10.1016/j.ibiod.2017.04.016.

[7] K. Sujarit, W. Pathom-aree, M. Mori, K. Dobashi, K. Shiomi, and S. Lumyong, “Streptomyces palmae CMU-AB204T, an antifungal producing-actinomycete, as a potential biocontrol agent to protect palm oil producing trees from basal stem rot disease fungus, Ganoderma boninense,” Biol. Control, vol. 148, no. May, p. 104307, 2020. https://doi.org/10.1016/j.biocontrol.2020.104307.

[8] Hamdani, A. Septiarini, and D. M. Khairina, “Model assessment of land suitability decision making for oil palm plantation,” in Int. Conf. Sci. Inf. Technol. ICSITech, 2017, pp. 109–113. https://doi.org/10.1109/ICSITech.2016.7852617.

Vol. 7, No. 3, June 2026, Page. 2588-2599
https://jutif.if.unsoed.ac.id
DOI: https://doi.org/10.52436/1.jutif.2026.7.3.5554

[9] A. Nasiri, A. Taheri-Garavand, and Y. D. Zhang, "Image-based deep learning automated sorting of date fruit," Postharvest Biol. Technol., vol. 153, no. January, pp. 133–141, 2019. https://doi.org/10.1016/j.postharvbio.2019.04.003.

[10] N. M. Trieu and N. T. Thinh, "A Study of Combining KNN and ANN for Classifying Dragon Fruits Automatically," Journal of Image and Graphics, vol. 10, no. 1, pp. 28–35, 2022. https://doi.org/ 10.18178/joig.10.1.28-35.

[11] D. M. Asriny, S. Rani, and A. F. Hidayatullah, "Orange Fruit Images Classification using Convolutional Neural Networks," IOP Conf. Ser. Mater. Sci. Eng., vol. 803, no. 1, 2020. https://doi.org/10.1088/1757-899X/803/1/012020.

[12] A. Y. Khaled, S. Abd Aziz, S. K. Bejo, N. M. Nawi, and I. Abu Seman, "Spectral features selection and classification of oil palm leaves infected by Basal stem rot (BSR) disease using dielectric spectroscopy," Comput. Electron. Agric., vol. 144, no. August 2017, pp. 297–309, 2018. https://doi.org/10.1016/j.compag.2017.11.012

[13] A. Septiarini, H. Hamdani, E. Junirianto, M. S. S. Thayf, G. Triyono, and Henderi, "Oil Palm Leaf Disease Detection on Natural Background Using Convolutional Neural Networks," in IEEE International Conference on Communication, Networks and Satellite (COMNETSAT), 2022, pp. 388– 392. https://doi.org/ 10.1109/COMNETSAT56033.2022.9994555.

[14] Ü. Atila, M. Uçar, K. Akyol, and E. Uçar, "Plant leaf disease classification using EfficientNet deep learning model," Ecol. Inform., vol. 61, no. October 2020, p. 101182, 2021. https://doi.org/10.1016/j.ecoinf.2020.101182.

[15] D. Kholiya, A. K. Mishra, A. Dumka, N. K. Pandey, and N. Tripathi, "Detection of Leaf Diseases in Agricultural Plants Using Machine Learning," in 2023 International Conference on Computer, Electronics & Electrical Engineering & their Applications (IC2E3), 2023, pp. 1–7. https://doi.org/10.1109/IC2E357697.2023.10262807.

[16] A. Alpyssov et al., "Assessment of Plant Disease Detection By Deep Learning," Eastern-European J. Enterp. Technol., vol. 1, no. 2–121, pp. 41–48, 2023. https://doi.org/10.15587/1729-4061.2023.274483.

[17] A. M. Roy and J. Bhaduri, "A Deep Learning Enabled Multi-Class Plant Disease Detection Model Based on Computer Vision," AI, vol. 2, no. 3, pp. 413–428, 2021. https://doi.org/10.3390/ai2030026.

[18] S. V Militante, B. D. Gerardo, and N. V Dionisio, "Plant Leaf Detection and Disease Recognition using Deep Learning," in IEEE Eurasia Conference on IOT, Communication and Engineering (ECICE), 2019, pp. 579–582. https://doi.org/10.1109/ECICE47484.2019.8942686.

[19] W. P. Siraskar, K. H. Gudadhe, and R. K. Mahajan, "Plant Disease Detection using an Image Processing Technique and Machine Learning," in 14th Int. Conf. Adv. Comput. Control. Telecommun. Technol. ACT, 2023, pp. 1557–1560. https://doi.org/10.37896/jxu14.7/012.

[20] J. H. Ong, P. Ong, and W. K. Lee, "Image-based Oil Palm Leaf Disease Detection using Convolutional Neural Network," J. Inf. Commun. Technol., vol. 21, no. 3, pp. 383–410, 2022. https://doi.org/10.32890/jict2022.21.3.4.

[21] Y. Nuwara, W. K. Wong, and F. H. Juwono, "Modern Computer Vision for Oil Palm Tree Health Surveillance using YOLOv5," in International Conference on Green Energy, Computing and Sustainable Technology (GECOST), pp. 404–409, 2022. https://doi.org/10.1109/GECOST55694.2022.10010668.

[22] A. Septiarini, H. Hamdani, S. U. Sari, H. R. Hatta, N. Puspitasari, and W. Hadikurniawati, "Image Processing Techniques For Tomato Segmentation Applying K-Means Clustering and Edge Detection Approach," in International Seminar on Machine Learning, Optimization, and Data Science (ISMODE), pp. 92–96, 2022. https://doi.org/ 10.1109/ISMODE53584.2022.9742740.

[23] X. Bi, C. Shuai, B. Liu, B. Xiao, W. Li, and X. Gao, "Privacy-Preserving Color Image Feature Extraction by Quaternion Discrete Orthogonal Moments," IEEE Trans. Inf. Forensics Secur., vol. 17, pp. 1655–1668, 2022. https://doi.org/10.1109/TIFS.2022.3170268.

[24] Y. Deng and Y. Yu, "Self-feedback image retrieval algorithm based on annular color moments," Eurasip J. Image Video Process., vol. 2019, no. 1, 2019. https://doi.org/10.1186/s13640-018-0400-9.

Vol. 7, No. 3, June 2026, Page. 2588-2599
https://jutif.if.unsoed.ac.id
DOI: https://doi.org/10.52436/1.jutif.2026.7.3.5554

[25] A. Septiarini, R. Saputra, A. Tejawati, M. Wati, and H. Hamdani, "Pattern Recognition of Sarong Fabric Using Machine Learning Approach Based on Computer Vision for Cultural Preservation," International Journal of Intelligent Engineering and Systems, no. 15, vo. 5, 2022. https://doi.org/10.22266/ijies2022.1031.26.

[26] K. Hameed, D. Chai, and A. Rassau, "A comprehensive review of fruit and vegetable classification techniques," Image Vis. Comput., vol. 80, pp. 24–44, 2018. https://doi.org/10.1016/j.imavis.2018.09.016.

[27] F. Kitzler, H. Wagentristl, R. W. Neugschwandtner, A. Gronauer, and V. Motsch, "Influence of Selected Modeling Parameters on Plant Segmentation Quality Using Decision Tree Classifiers," Agriculture, no. 12, vo. 9, 2022. https://doi.org/10.3390/agriculture12091408.

[28] A. Razafinimaro, A. R. Hajalalaina, H. Rakotonirainy, and R. Zafimarina, "Land cover classification based optical satellite images using machine learning algorithms," Int. J. Adv. Intell. Informatics, vol. 8, no. 3, pp. 362–380, 2022. https://doi.org/10.26555/ijain.v8i3.803

[29] E. Winarno, W. Hadikurniawati, A. Septiarini, and H. Hamdani, "Analysis of color features performance using support vector machine with multi-kernel for batik classification," Int. J. Adv. Intell. Informatics, vol. 8, no. 2, pp. 151–164, 2022. https://doi.org/10.26555/ijain.v8i2.821.

[30] D. Rahadiyan, S. Hartati, Wahyono, and A. P. Nugroho, "Feature aggregation for nutrient deficiency identification in chili based on machine learning," Artif. Intell. Agric., vol. 8, pp. 77–90, 2023. https://doi.org/10.1016/j.aiia.2023.04.001.

[31] A. Septiarini, H. Hamdani, and D. M. Khairina, "The contour extraction of cup in fundus images for glaucoma detection," International Journal of Electrical and Computer Engineering, vol. 6, no. 6, pp. 2797–2804, 2016. http://doi.org/10.11591/ijece.v6i6.pp2797-2804.